

Modeling of the processes of ionization and excitation of nitrogen molecules by short and intense laser pulses

Vladimir T. Tikhonchuk ^{1,2,*} Yi Liu ^{3,4} Rostyslav Danylo ^{5,3} Aurélien Houard ⁵ and André Mysyrowicz ⁵

¹University of Bordeaux-CNRS-CEA, Centre Lasers Intenses et Applications, UMR 5107, 33405 Talence, France

²ELI-Beamlines Center, Institute of Physics, Czech Academy of Sciences, 25241 Dolní Břežany, Czech Republic

³Shanghai Key Lab of Modern Optical System, University of Shanghai for Science and Technology, Shanghai 200093, China

⁴CAS Center for Excellence in Ultra-intense Laser Science, Shanghai 201800, China

⁵Laboratoire d'Optique Appliquée, ENSTA Paris, CNRS, Ecole Polytechnique, Institut Polytechnique de Paris, 91762 Palaiseau, France



(Received 28 September 2021; accepted 26 November 2021; published 20 December 2021)

We present a model describing ionization and excitation of nitrogen molecules by a strong and short laser pulse. Different from previous publications, both processes are considered within the same formalism of the density matrix. We account for the dependence of the dipole moment on the vibrational quantum number and for a large number of excited levels. Populations of the excited levels depend significantly on the laser intensity, wavelength, polarization, and pulse duration.

DOI: [10.1103/PhysRevA.104.063116](https://doi.org/10.1103/PhysRevA.104.063116)

I. INTRODUCTION

Cavity-free lasing of nitrogen singly ionized molecules was reported for the first time 10 years ago [1,2] and attracted the attention of many research groups [3–9]. The effect consists of lasing in the forward direction at a wavelength of 391 or 428 nm, corresponding to transitions from the excited state $B^2\Sigma_u^+$ to the ground states $X^2\Sigma_g^+(0, 1)$ of the N_2^+ molecule with vibrational levels 0 and 1, respectively. There is still ongoing controversy over how this lasing is produced because, owing to the very short duration of the laser pump pulse, typically less than 50 fs, it is not known whether population inversion between B and X states can be created.

This controversy over the explanation of the lasing effect is due to the fact that the nitrogen molecule is a complex quantum object and only a limited number of excited levels are usually considered. The challenge consists of evaluating the probability of excitation of different electronic and vibrational levels after the end of the laser pulse. Only if we know the populations in all relevant levels would it be possible to define the origin of the lasing process. The probability of direct laser ionization into excited state B is very low compared to ionization into ground state $X0$ because of the large difference in energies and the low probability of electron recollision [10,11]. However, three other processes may contribute to the observed lasing effect. The first process is the excitation to a third level, A . There is an intermediate state, $A^2\Pi_u$, between the X and B states that can be resonantly excited by a pump pulse at wavelength ~ 800 nm because the transition energy between the $X0$ and $A2$ levels, $\hbar(\omega_{a2} - \omega_{x0}) = 1.59$ eV, is very close to the pump photon energy, $\hbar\omega_0 = 1.55$ eV. Thus, a transition of a fraction of ionized molecules to the A state may create a population inversion between the B and X states

and explain the lasing effect [5,6]. However, this scheme assumes a population inversion between the A and X states, which is not evidenced experimentally and is not found in the numerical modeling [12]. A second process is the polarization coupling between the B and A states [13]. This process, also known as the V scheme [14–16], can explain the lasing effect without population inversion [12,13,17–20]. The third process is the population inversion between rotational levels of the B and X states because of coherent reconstruction of the rotational wave packet of N_2^+ ions [9,21]. Indeed, ionization of nitrogen molecules is accompanied by coherent excitation of many rotational levels. The periodic partial alignment of the molecular ions results in a transient inversion between certain rotational B and X levels that may explain the lasing effect [22,23]. However, such an inversion exists only for short time periods of molecular alignment separated by half of a period of molecular rotations, which is equal to approximately 4 ps.

In our previous paper [12], we considered a model of the nitrogen molecular ion N_2^+ including the ground electronic state $X^2\Sigma_g^+$ with two vibrational levels, $v = 0, 1$, and two excited electronic levels: the first excited state $A^2\Pi_u$, with vibrational levels $v = 2, 3$, and the second excited state $B^2\Sigma_u^+$, with vibrational level $v = 0$. The model was simplified by assuming a limited number of allowed transitions; namely, four transitions were considered, $A2-X0$, $A3-X1$, $B0-X0$, and $B0-X1$, and two $A-X$ and two $B-X$ transitions were characterized by the same dipole moments, $\mu_{ax} = 0.25ea_B$ and $\mu_{bx} = 0.75ea_B$ [24,25], where e is the unitary charge and a_B is the Bohr radius. This choice of transitions was justified by the resonance conditions as the frequencies of the $A2-X0$ and $A3-X1$ transitions are close to the laser frequency.

Although this model goes beyond the traditional three-level scheme [5,6], it is not known how well this simplified five-level model corresponds to reality as the nitrogen ion has many more vibrational levels and many more cross couplings

*tikhonchuk@u-bordeaux.fr

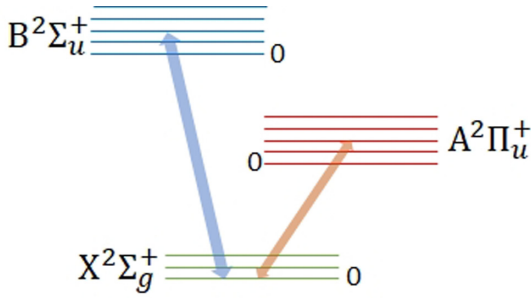


FIG. 1. Scheme of electronic and vibrational levels in the molecule N_2^+ . The number of lines indicates the number of vibrational levels considered; rotational splitting is neglected. Arrows show the allowed transitions.

are allowed. A recent study by Zhang *et al.* [26] showed the possibility of efficient excitation of higher vibrational B levels. In the present work we extend the ionization-excitation model by revising the ionization model of the nitrogen molecule, including more vibrational levels at the X and A states and accounting for all allowed transitions between the considered levels shown in Fig. 1. We consider the dependence of dipole moments on the vibrational quantum number by using experimental values for the Einstein coefficients for transitions and Franck-Condon coefficients for ionization [24,25,27,28].

A comparison of the populations of involved states for realistic laser-pulse parameters shows that it is necessary to account for three to five vibrational levels in each electronic state in order to have convergent results. The calculated populations are significantly different from the simplified three- and five-level models and from the calculation of populations using the equations for the probability amplitudes [5,7].

II. ELEMENTS OF THE THEORETICAL MODEL

Our model is based on the Bloch equations for the density matrix of a nitrogen molecule in a prescribed strong, time-dependent laser field. Different from equations for the complex probability amplitudes, which describe only transitions between discrete levels, equations for the density matrix may also include the terms describing the molecule ionization into the ground and excited ionic states. Thus, the use of equations for the density matrix allows one to account for both ionization and excitation processes self-consistently, which cannot be done with the equations for the probability amplitudes.

Some authors [5,7,29] have proposed to associate ionization with the maximum of the laser pulse and then to solve the amplitude equations for the second half of the pulse for the evaluation of population in the excited levels. However, our analysis shows that such a scheme is inconsistent with the density-matrix approach, showing quantitatively different results for the ionization level and populations in excited states.

The dynamic equation for the density matrix \mathbf{d} has a standard form [12,26,30]:

$$\dot{\mathbf{d}} = -\frac{i}{\hbar}[\mathbf{H}, \mathbf{d}] + (1 - n_i)\mathbf{w}_{fi}, \quad (1)$$

where the Poisson brackets in the first term on the right-hand side describe transitions between the ground and excited states of the ion and the second term describes ionization of the nitrogen molecule to the ground and excited states. The density matrix is normalized to the density of neutral molecules. Then, the trace of \mathbf{d} gives the total probability of ionization $n_i = \text{Tr } \mathbf{d}$. According to Eq. (1), it satisfies the equation

$$\dot{n}_i = (1 - n_i)\text{Tr } \mathbf{w}_{fi}. \quad (2)$$

The ionization matrix \mathbf{w}_{fi} is diagonal and represents the probability of ionization to the corresponding levels.

The Hamiltonian $\mathbf{H} = \mathbf{H}^0 - \boldsymbol{\mu} \cdot \mathbf{E}(t)$ is assumed to be Hermitian, with the diagonal term $\mathbf{H}^0 = \hbar\boldsymbol{\omega}$ representing the energies of the ground and excited states and the off-diagonal term $\boldsymbol{\mu} \cdot \mathbf{E} = \hbar\boldsymbol{\Omega}$ representing the dipole interaction between levels, with $\boldsymbol{\Omega}$ being the Rabi frequency. Explicit expressions for the ionization and dipole matrices for the 13 considered levels and 29 transitions are presented in the next sections.

We consider excited electronic states of the nitrogen molecular ion $A^2\Pi_u$ and $B^2\Sigma_u^+$ corresponding to the value of the dominant orbital quantum number $l = 1$ and magnetic quantum numbers (projection of the orbital momentum on the molecular axis) $m = 0$ (B state) and $m = \pm 1$ (A state). Each of these states, as well as the ground state $X^2\Sigma_g^+$, includes many vibrational levels. We consider three vibrational levels in the ground state X , $v = 0-2$; five levels in the A state, $v = 0-4$; and five levels, $v = 0-4$, in the B state, which correspond to 29 transitions in the optical and near-infrared range. The wavelengths of the considered transitions along with the corresponding Einstein coefficients are given in Table I and described in the Appendix. In particular, the wavelengths of transitions $A2-X0$ and $A3-X1$ are very close to the laser wavelength of 800 nm used in many experiments, and the wavelengths of transitions $B0-X0$ and $B0-X1$ are close to its second harmonic. Comparing our method to that of Zhang *et al.* [26], we omitted higher-order vibrational levels $v = 3, 4$ in the X state as their populations are expected to be quite small, less than 0.1%.

Expressions for the dipole interaction depend on the laser-pulse polarization. In the case of linear polarization, interaction depends on the angle Θ between the directions of the electric field and molecule's axis. We consider a laser field directed along the x axis in the form

$$E_x(t) = E_0 \cos(\omega_0 t) \cos(\pi t/2t_{\text{las}}) H(t_{\text{las}} - |t|), \quad (3)$$

where E_0 is the laser amplitude, ω_0 is the laser frequency, t_{las} is the laser-pulse duration at half the maximum intensity, and H is the Heaviside function. The Rabi frequencies for the $B-X$ and $A-X$ transitions read

$$\hbar\Omega_{BX} = \mu_{BX} E_x \cos \Theta, \quad (4)$$

$$\hbar\Omega_{AX} = \mu_{AX} E_x \sin \Theta, \quad (5)$$

where \hbar is Planck's constant. Considering a laser-pulse duration on a tens of femtoseconds scale, which is much smaller than the period of molecular rotation (~ 8 ps), we average the density matrix at the end of the laser pulse over the molecular orientation with respect to the laser field direction, assuming there is no privileged orientation before the

TABLE I. Wavelengths λ_{ab} , the corresponding Einstein coefficients A_{ab} , frequencies, and dipole moments for transitions AX and BX of the molecular ion N_2^+ . Here, $\omega_{at} = v_{at}/a_B$ is the atomic frequency, and $v_{at} = e^2/4\pi\epsilon_0\hbar$ is the atomic velocity; μ_{ab} is calculated from Eq. (A1) using the Einstein coefficients given in Refs. [24,25,27,28].

Transition	λ_{ab} (nm)	A_{ab} (s^{-1})	ω_{ab}/ω_{at}	μ_{ab}/ea_B
A0-X0	1108.7	4.63×10^4	0.0415	0.249
A0-X1	1461.0	1.46×10^4	0.0315	0.211
A0-X2	2126.5	1.37×10^3	0.0216	0.114
A1-X0	918.15	5.70×10^4	0.0501	0.208
A1-X1	1147.2	3.17×10^3	0.0401	0.068
A1-X2	1521.1	1.17×10^4	0.0302	0.201
A2-X0	785.25	3.86×10^4	0.0585	0.135
A2-X1	946.69	3.68×10^4	0.0486	0.175
A2-X2	1188.0	1.32×10^3	0.0387	0.047
A3-X0	687.36	1.94×10^4	0.0669	0.079
A3-X1	808.18	5.27×10^4	0.0569	0.165
A3-X2	977.40	1.25×10^4	0.0470	0.107
A4-X0	612.30	8.17×10^3	0.0751	0.043
A4-X1	706.37	4.13×10^4	0.0651	0.119
A4-X2	832.31	4.30×10^4	0.0552	0.156
B0-X0	391.44	1.24×10^7	0.1175	0.854
B0-X1	427.81	3.70×10^6	0.1075	0.533
B0-X2	470.92	7.34×10^5	0.0976	0.274
B1-X0	358.21	5.86×10^6	0.1283	0.514
B1-X1	388.43	4.87×10^6	0.1084	0.529
B1-X2	423.65	4.40×10^6	0.1085	0.572
B2-X0	330.80	7.90×10^5	0.1390	0.167
B2-X1	356.39	8.25×10^5	0.1290	0.605
B2-X2	385.79	1.50×10^6	0.1192	0.291
B3-X0	307.82	2.02×10^4	0.1494	0.024
B3-X1	329.87	1.77×10^6	0.1394	0.250
B3-X2	354.89	8.80×10^6	0.1295	0.621
B4-X1	307.64	6.23×10^4	0.1494	0.042
B4-X2	329.34	2.35×10^6	0.1396	0.287

laser arrival. The spatial dependence of the laser field is not considered in this model as the laser pulse is assumed to be sufficiently strong and weakly modified while propagating in the gas. Consequently, all molecules are ionized and excited synchronously with the laser-pulse propagation. The intensity in the calculations below corresponds to the maximum value, $I_{\text{las}} = \frac{1}{2}c\epsilon_0 E_0^2$.

The calculation of the molecule ionization and excitation becomes more complicated if the laser polarization changes direction within the pulse duration. Here, we consider a laser wave with elliptic polarization propagating in the z direction with the electric field \mathbf{E} in the x, y plane composed of two linear polarizations, $\mathbf{E}(t) = \mathbf{x}E_x(t) + \mathbf{y}E_y(t)$, defined by unit vectors \mathbf{x} and \mathbf{y} , with the phases shifted by a quarter of the period:

$$E_x(t) = E_0 \cos \beta \cos(\omega_0 t) \cos(\pi t/2t_{\text{las}}) H(t_{\text{las}} - |t|), \quad (6)$$

$$E_y(t) = E_0 \sin \beta \sin(\omega_0 t) \cos(\pi t/2t_{\text{las}}) H(t_{\text{las}} - |t|). \quad (7)$$

A difference in amplitudes, E_{0x} and E_{0y} , is controlled by the angle β , and ellipticity is defined as $\epsilon = \tan \beta$.

Molecule orientation is characterized by a unit vector \mathbf{n} , which in spherical coordinates is defined by the polar angle θ_n with respect to the laser propagation direction z and the azimuthal angle ψ_n in the laser polarization plane x, y . The absolute value of the laser electric field and the angle between the molecule orientation and laser field can be presented as

$$E_{\text{abs}}(t) = (E_x^2 + E_y^2)^{1/2}, \quad (8)$$

$$\cos \Theta = \sin \theta_n \left(\cos \psi_n \frac{E_x}{E_{\text{abs}}} + \sin \psi_n \frac{E_y}{E_{\text{abs}}} \right). \quad (9)$$

Rabi frequencies for $B-X$ transitions, with orbitals that have zero projection on the molecular axis, are given by Eq. (4) with the field E_x replaced by E_{abs} . More attention is required for the definition of Rabi frequencies for the $A-X$ transitions, which correspond to a change in the projection of the orbital momentum to the molecular axis $\Delta m = \pm 1$. Here, there are two probability amplitudes corresponding to left- and right-hand rotations. They are coupled to the corresponding field amplitudes $E^\pm = 2^{-1/2}(E_x \pm iE_y)$, which are defined in the coordinate system where the molecular axis \mathbf{n} is oriented along the z' axis. We define the y' axis by a unit vector directed perpendicular to the plane defined by the z axis and the molecular axis: $\mathbf{y}' = \mathbf{z} \times \mathbf{n} / \sin \theta_n$. Then, the third direction in this system, \mathbf{x}' , is defined as a vector product, $\mathbf{x}' = \mathbf{y}' \times \mathbf{n}$. Consequently, the field components in the molecule reference system are defined by the following relations:

$$E^\pm = 2^{-1/2} E_x \mathbf{x} \cdot (\mathbf{x}' \pm i\mathbf{y}') + 2^{-1/2} E_y \mathbf{y} \cdot (\mathbf{x}' \pm i\mathbf{y}'). \quad (10)$$

In the particular case of time-independent laser polarization, we can assume that two vectors, laser polarization and molecule orientation, are lying in the x, z plane, and then $\cos \Theta = \sin \theta_n$, and $E^\pm = E \cos \theta_n$. In a more general case, the Rabi frequencies are also split into left and right components:

$$\hbar\Omega_{AX}^\pm = \mu_{AX} E^\mp. \quad (11)$$

This matrix is Hermitian: $\Omega_{AX}^+ = \Omega_{AX}^{-*}$.

A. Dipole moments of electronic and vibrational transitions

The transition wavelengths λ_{ab} and the corresponding Einstein coefficients A_{ab} are given in Table I and described in the Appendix. The dipole moments are related to the Einstein coefficients as follows [31]:

$$\mu_{ab}^2 = \frac{3\hbar\epsilon_0}{16\pi^2} \lambda_{ab}^3 A_{ab}, \quad (12)$$

where ϵ_0 is the vacuum dielectric permittivity.

Dipole moments for $B-X$ transitions shown in Table I are significantly larger than those for $A-X$ transitions. This leads to a larger population in B levels and a smaller population in A levels, which favors the subsequent amplification in the V scheme. Dipole moments for the considered states depend on the vibrational quantum number. This fact was not accounted for in previous publications [5,12,29], which leads to quantitative differences in the populations of excited levels.

TABLE II. Coefficients for N₂ molecule ionization in the ground and excited states [26] and Franck-Condon ionization factors [28].

N ₂ ⁺ orbital	<i>l</i>	<i>m</i>	<i>C_l</i>	<i>v</i>	<i>q_a^{FCi}</i>
X ² Σ _g ⁺	0	0	2.86	0	0.905
	2	0	1.37	1	0.089
	4	0	0.21	2	0.006
A ² Π _u	1	±1	3.06	0	0.275
	3	±1	0.21	1	0.320
				2	0.215
				3	0.111
B ² Σ _u ⁺	1	0	4.23	0	0.886
	3	0	0.83	1	0.111
				2	0.002
				4	0.049

B. Ionization probability

Ionization of the nitrogen molecules is described by the model developed in Refs. [32–34] and adapted for diatomic molecules by Tong *et al.* [35]. Ionization probability to level *a* is characterized by the ionization potential *U_a* and reads

$$w_{a,\text{fi}} = \omega_{\text{at}} \frac{q_a^{\text{FCi}} B_a^2}{2^{|m|} |m|!} \kappa_a^{1-2/\kappa_a} \left(\frac{2\kappa_a^3}{F} \right)^{2/\kappa_a - |m| - 1} \exp\left(\frac{2\kappa_a^3}{3F} \right). \quad (13)$$

Here, *m* is the projection of the orbital moment on the molecular axis, $\kappa_a = (2U_a/\hbar\omega_{\text{at}})^{1/2}$ and $F = E_{\text{abs}}/E_{\text{at}}$ are the ionization energy and electric field expressed in atomic units, $\omega_{\text{at}} = e^2/4\pi\epsilon_0 a_B \hbar$, $E_{\text{at}} = \hbar\omega_{\text{at}}/ea_B$, q_a^{FCi} is the Franck-Condon ionization factor [28], and coefficient *B_a* is expressed as

$$B_a(m, \Theta) = \sum_{l,m'} C_l D_{m',m}^{(l)} Q(l, m'), \quad (14)$$

where $Q(l, m) = (-1)^m [(2l+1)(l+|m|)!/2(l-|m|)!]^{1/2}$ are the numerical coefficients and $D_{m',m}^{(l)}(\Theta)$ is the matrix of rotation [36] depending on the angle Θ between the directions of the electric field and molecular axis. The coefficients *C_l* are provided in Zhang *et al.*'s Supplementary Material [26] and are given in Table II.

The angular dependence of the ionization probability is defined by the expression for the coefficients *B_a(m, Θ)* given by Eq. (14). Following Table II, we assume that two orbitals, *l* = 0 and *l* = 2, contribute to the ground state *X*. For *A* and *B* states, it is sufficient to account for one orbital, *l* = 1. Consequently, by using data from Table II, the following expressions for coefficients *B* can be found: $B_X \simeq 1 + 3 \cos^2 \Theta$, $B_A \simeq 5.3$, and $B_B \simeq 5.2 \cos \Theta$. This angular dependence of the ionization is in qualitative agreement with the experimental results presented in Ref. [37].

This ionization model predicts, however, too high ionization probability compared to experiments [38]. This can be explained by the radial distribution of the laser-pulse intensity in the experiment: the gas ionization averaged in the direction transverse to the propagation axis is smaller than at the axis. Agreement with the experiment can be achieved by reducing all ionization probabilities in Eq. (13) by a numerical factor of 10. With this correction, as shown in Fig. 2(a), we find

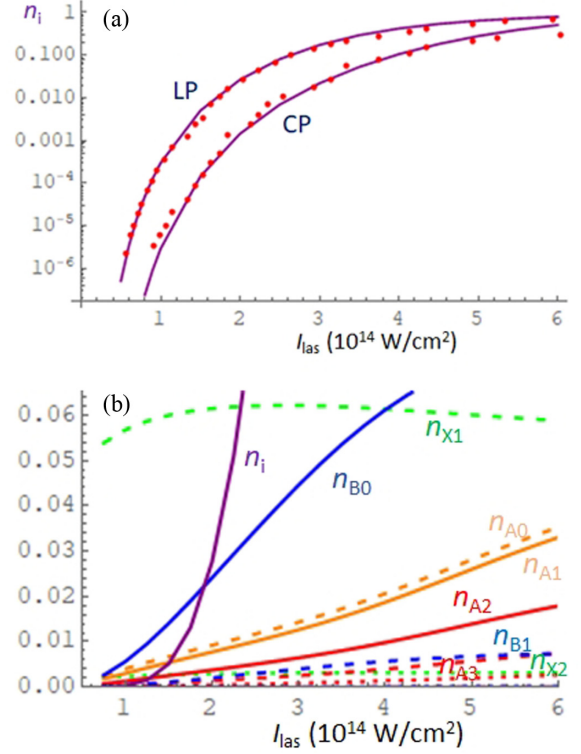


FIG. 2. (a) Dependence of the total ionization probability n_i on the laser intensity. Solid lines represent calculations with our model for linear (LP) and circular (CP) laser polarizations. Points show the corresponding experimental results from Ref. [38]. (b) Dependence of populations in excited states X1 (green long-dashed line), X2 (green dotted line), A0 (orange dashed line), A1 (orange solid line), A2 (red solid line), A3 (red dashed line), A4 (red dotted line), B0 (blue solid line), B1 (blue dashed line), and B2 (blue dotted line) normalized to the total ion density on the laser intensity for a laser-pulse duration of 30 fs and a laser wavelength of 800 nm. Results were obtained by solving equations for the density matrix (1) for 13 levels without polarization coupling between levels. The population in level X0, which is on the order of 90%, is not shown.

good agreement of the angle-averaged ionization probability in the range of laser intensity of $(0.5\text{--}6) \times 10^{14}$ W/cm² with the experimental data given by Guo *et al.* [38] for a laser-pulse duration of 30 fs FWHM. Experimental data are normalized by a factor of 3.5×10^{-8} and shifted on intensity by 1.4×10^{13} W/cm². (This shift is within the precision of the intensity definition in the experiment.) Agreement is also good for the circular laser polarization with the same scaling and shift factor as the linear polarization. This close agreement gives us confidence in considering the populations in excited states. Since the excitation probabilities do not depend on the absolute number of ionized molecules, we use this ionization suppression factor of 0.1 in all calculations presented in below.

Figure 2(b) shows the distribution of populations in the excited states as a function of laser intensity for the same pulse duration of 30 fs. Ionization to the ground state dominates, with the fraction of ions decreasing from 93% at low intensity

TABLE III. Comparison of the populations in the ground and excited levels calculated with the model presented in Ref. [26] and our model for the cases without polarization coupling (N) and with polarization coupling (P). Laser intensity is 3×10^{14} W/cm², wavelength is 800 nm, and pulse duration is 30 fs. The abbreviations 45° and Avr. denote our calculations for $\Theta = 45^\circ$ and angle-averaged ionization, respectively, for the same conditions.

Model		Level									
		X0	X1	X2	A0	A1	A2	A3	B0	B1	B2
N	[26]	0.560	0.049	0.	0.066	0.081	0.057	0.030	0.005	0	0
	45°	0.773	0.057	0.003	0.064	0.057	0.029	0.012	0	0	0
	Avr.	0.836	0.062	0.003	0.017	0.015	0.008	0.003	0.050	0.004	0
P	[26]	0.064	0.058	0.019	0.141	0.174	0.186	0.059	0.084	0.023	0.009
	45°	0.043	0.087	0.016	0.056	0.061	0.075	0.042	0.095	0.191	0.091
	Avr.	0.097	0.164	0.027	0.036	0.053	0.130	0.046	0.067	0.161	0.111

to about 78% at high intensity. Populations of all excited states are low and follow the inverse order to the ionization energy. Figure 2(b) demonstrates that direct ionization into excited states cannot produce inversion of the population and cannot explain the lasing effect. Coupling between levels changes the situation completely.

The results of our ionization model can be compared with the population calculations performed by Zhang *et al.* [26] for a laser intensity of 3×10^{14} W/cm², wavelength of 800 nm, and pulse duration of 30 fs and for a particular angle of molecule orientation with respect to the laser polarization of 45°. Zhang *et al.* used a similar theoretical model based on the solution of Eq. (1) for the density matrix. A comparison is shown in Table III. In the case without polarization coupling, there is qualitative agreement in the predicted populations for molecule orientation at 45°. Differences are more significant in the case where the populations are averaged over the molecule orientation and the polarization coupling is turned on. This is important for levels X0, A2, and B0, which are of particular interest for amplified emission at a wavelength of 391 nm, corresponding to the B0-X0 transition [13].

III. IONIZATION-EXCITATION MODEL

A. Dependence on the number of excited levels

Bloch equations (1) and (2) are solved numerically; ion state probabilities are evaluated at the end of the laser pulse, $t = 2t_{\text{las}}$, and averaged over the angle Θ assuming random orientation of the molecules with respect to the laser electric field. Figure 3(a) shows the dependence of populations in the excited levels on the laser intensity for a pulse duration of 30 fs, a wavelength of 800 nm, and linear polarization obtained with the model including 13 levels. Populations are strongly enhanced and reversed due to the polarization coupling compared to the case where only direct ionization is activated [Fig. 2(b)]. Compared to the five-level model [12], ions are distributed more equally between several excited levels, and populations oscillate as laser intensity increases.

Having in hand simulation results obtained with the model accounting for 13 levels and 29 transitions, we can now take a step back and evaluate the minimum number of levels and transitions needed for accurate calculation of populations. By suppressing transitions characterized by small values of the dipole moment, we conclude that all transitions going to level

X2 can be removed without significantly affecting populations in other levels. A similar observation applies to transitions going from levels A4, B3, and B4. In total 4 levels and 17 transitions can be suppressed in the model without affecting the populations in the remaining levels. Thus, the minimum

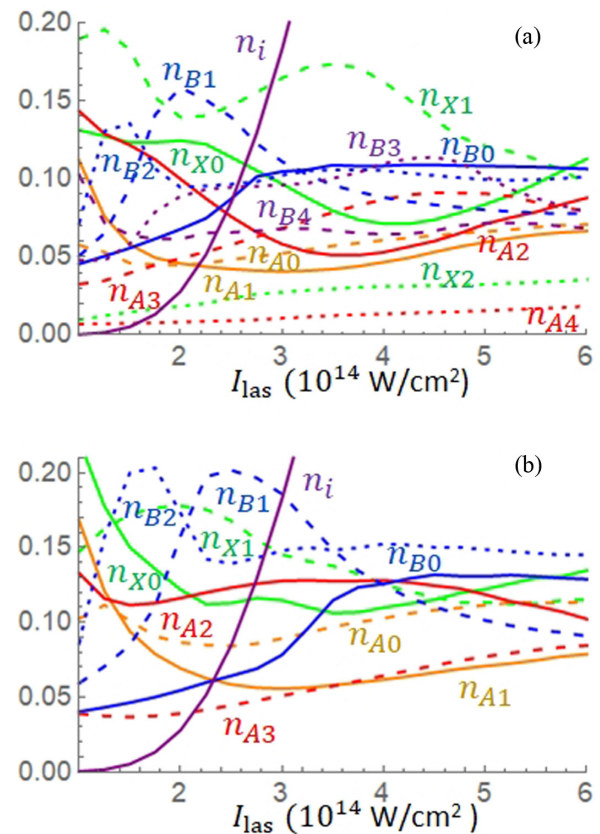


FIG. 3. Dependence of the populations in levels X0 (green solid line), X1 (green long-dashed line), X2 (green dotted line), A0 (orange dashed line), A1 (orange solid line), A2 (red solid line), A3 (red dashed line), A4 (red dotted line), B0 (blue solid line), B1 (blue dashed line), B2 (blue dotted line), B3 (purple dashed line), and B4 (purple dotted line) normalized to the total ion density n_i on the laser intensity for a laser-pulse duration of 30 fs and a wavelength of 800 nm. Total ionization probability n_i is shown by a solid purple line. Thirteen levels are considered in (a); four levels have been removed in (b): X2, A4, B3, and B4.

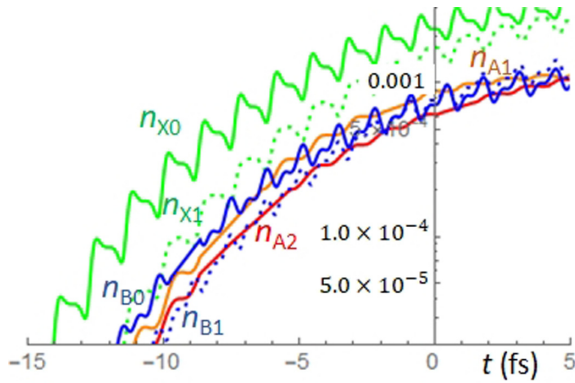


FIG. 4. Time dependence of the populations in states $X0$ (green solid line), $X1$ (green, dashed line), $A1$ (orange solid line), $A2$ (red solid line), $B0$ (blue solid line), and $B1$ (blue dashed line) normalized to the total density of neutral molecules. Laser intensity is 1.8×10^{14} W/cm 2 , pulse duration is 30 fs, wavelength is 800 nm, and angle $\Theta = 45^\circ$. Time $t = 0$ corresponds to the maximum of the laser intensity.

configuration includes two levels in the X state ($v = 0, 1$), four levels in the A state ($v = 0-3$), and three levels in the B state ($v = 0-2$). The dependence of populations on the laser intensity obtained with the reduced model is shown in Fig. 3(b). Qualitative agreement with the full model shown in Fig. 3(a) is evident, but there are quantitative differences that might be important for the evaluation of inversion of population between some particular levels.

This analysis also sheds light on how the levels are populated. Figure 4 shows an example of the temporal evolution of populations in several representative levels. Ionization populates essentially the $X0$ level. Level $X1$ is populated through the intermediary of the $B0$ level. So populations of both levels are comparable at early times. Depending on the laser parameters, this two-step transfer could be very efficient, with the population in the $X1$ level being at later times higher than populations in the $X0$ and B levels. Levels $A1$ and $A2$ are also populated from the $X0$ level, but their role in populating the $X1$ level is small in the case of linear laser polarization. By contrast, the roles of the B and A states are exchanged in the case of circular polarization. There, A levels mediate the transfer of ions to the $X1$ state, and populations in the B level are strongly reduced.

B. Linearly polarized laser pulse

Figure 5 shows the distribution of populations over all considered levels in more detail for a laser-pulse duration of 30 fs calculated with the full model including 13 levels. In the ground state X , there is an inversion between levels $X0$ and $X1$ in all considered interval of laser intensities, while the population in level $X2$ remains rather small, less than 3%. Populations in levels $A0-A3$ are of the same order of 5%–10%, while the population in level $A4$ is much smaller, less than 2%.

Populations in all levels in the B state are of the same order of 10% with notable variations at low intensities $I_{\text{las}} \lesssim$

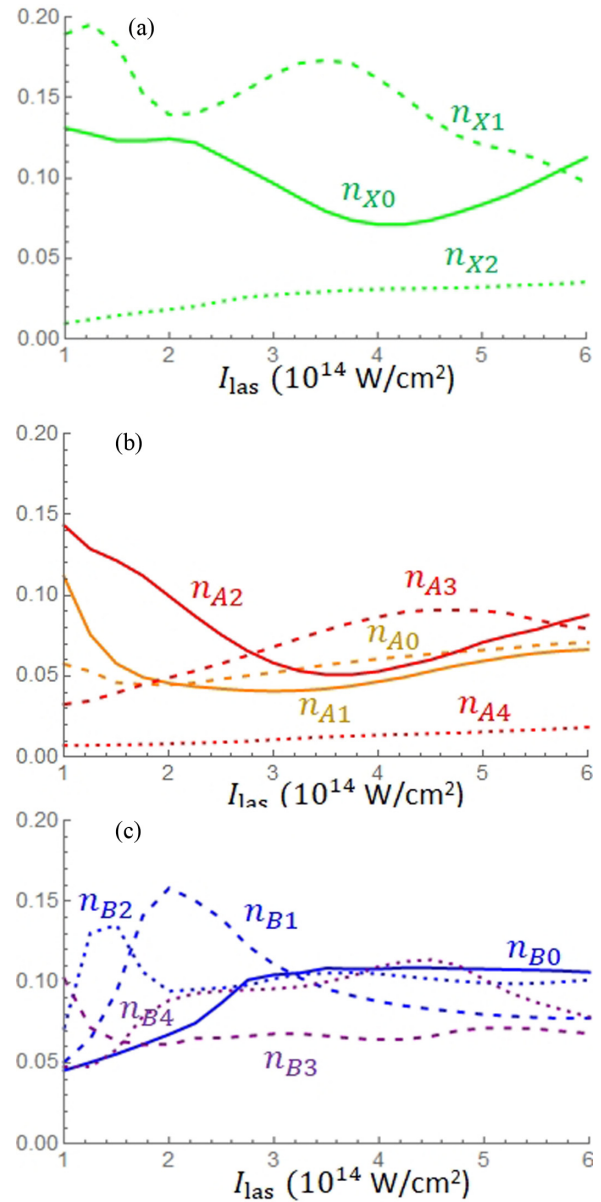


FIG. 5. Dependence of the populations in states (a) X , (b) A , and (c) B ; vibration levels are denoted as follows: $X0$ (green solid line), $X1$ (green dashed line), $X2$ (green dotted line), $A0$ (orange dashed line), $A1$ (orange solid line), $A2$ (red solid line), $A3$ (red dashed line), $A4$ (red dotted line), $B0$ (blue solid line), $B1$ (blue dashed line), $B2$ (blue dotted line), $B3$ (purple dashed line), and $B4$ (purple dotted line), normalized to the total ion density n_i on the laser intensity for a laser-pulse duration of 30 fs and a wavelength of 800 nm.

3×10^{14} W/cm 2 and approximately constant values at higher intensities.

Figure 6 shows populations in five levels of interest as a function of laser intensity for pulse durations of 10 and 50 fs. No inversion between populations in the $B0$ and $X0$ states is observed for a short laser pulse [Fig. 6(a)]. However, the population in level $X0$ gradually decreases with increasing pulse duration, and an inversion appears already at a pulse duration of 30 fs [see Figs. 3(a) and 5] and further increases at a pulse duration of 50 fs [Fig. 6(b)].

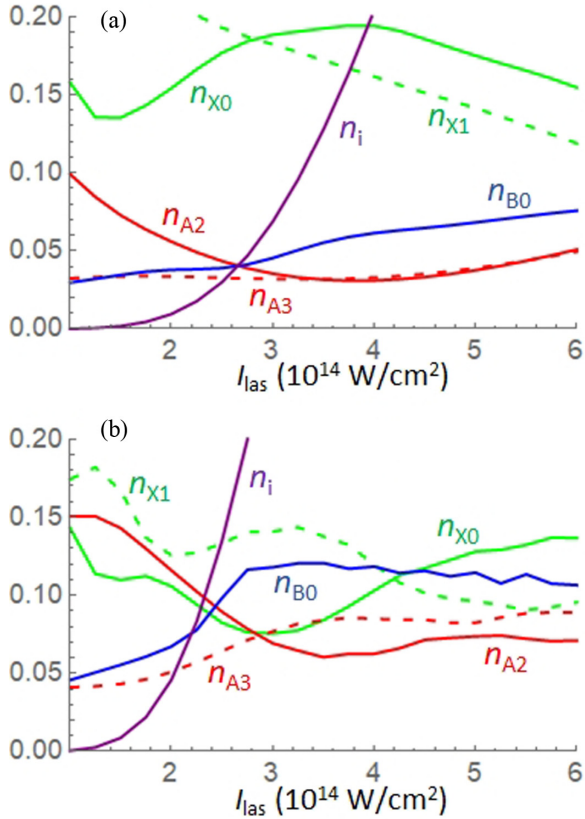


FIG. 6. Dependence of the populations in levels X0 (green solid line), X1 (green long-dashed line), A2 (red solid line), A3 (red dashed line), and B0 (blue solid line) normalized to the total ion density n_i on the laser intensity for a laser-pulse duration of (a) 10 and (b) 50 fs. Total ionization probability n_i is shown by a purple solid line. Laser wavelength is 800 nm.

The dependence of the populations in excited levels on laser wavelength is shown in Fig. 7. While the B0-X0 inversion is observed for a wavelength of 810 nm [Fig. 7(a)], the zone of inversion decreases as wavelength decreases, and it is completely suppressed for a wavelength of 780 nm for a pulse duration of 30 fs. This complicated variation of populations with respect to the laser intensity and wavelength can be explained by a variation of the energy difference between levels under the effect of the ponderomotive potential.

This analysis shows that inversion of populations between the B0 and X0 levels is unlikely to be the origin of the strong amplification of signals at wavelengths corresponding to the B0-X0 and B0-X1 transitions. By contrast, inversion between the B0 and A2 and A3 levels is observed in a large range of laser intensities, which favors the hypothesis of amplification in the three-level scheme [12,13].

C. Elliptically polarized laser pulse

Elliptical polarization of the laser pulse removes the degeneracy between transitions to the A levels with $m = 1$ and $m = -1$. Consequently, transitions to levels $A\nu^+$ and $A\nu^-$ should be considered separately. Figure 8 shows the temporal evolution of populations in the A levels for a circularly polarized laser pulse calculated with the model including 18

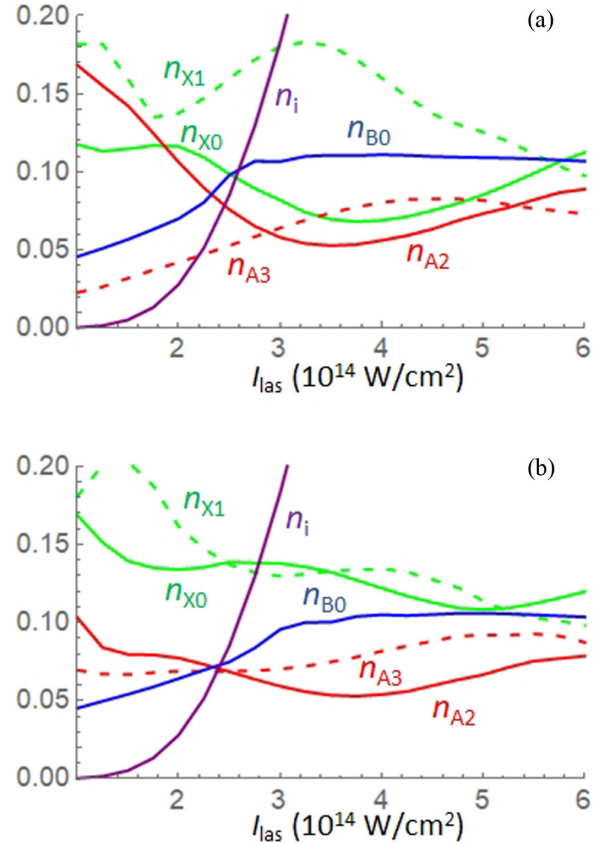


FIG. 7. Dependence of the populations in levels X0 (green solid), X1 (green long-dashed line), A2 (red solid line), A3 (red dashed line), and B0 (blue solid line) normalized to the total ion density n_i on the laser intensity for a laser wavelength of (a) 810 and (b) 780 nm. Total ionization probability n_i is shown by a purple solid line. Laser-pulse duration is 30 fs.

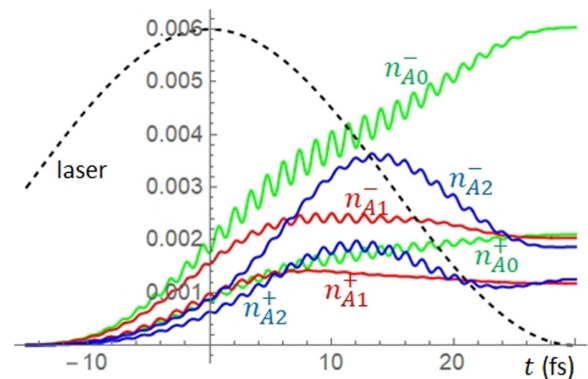


FIG. 8. Dependence of the populations in levels $A0^\pm$ (green solid line), $A1^\pm$ (red solid line), and $A2^\pm$ (blue solid line) on time for a laser intensity of 3×10^{14} W/cm 2 , a wavelength of 800 nm, and a pulse duration of 30 fs. The angles of molecule orientation are $\theta_n = 45^\circ$ and $\psi_n = 90^\circ$. The black dashed line shows the temporal evolution of the laser intensity.

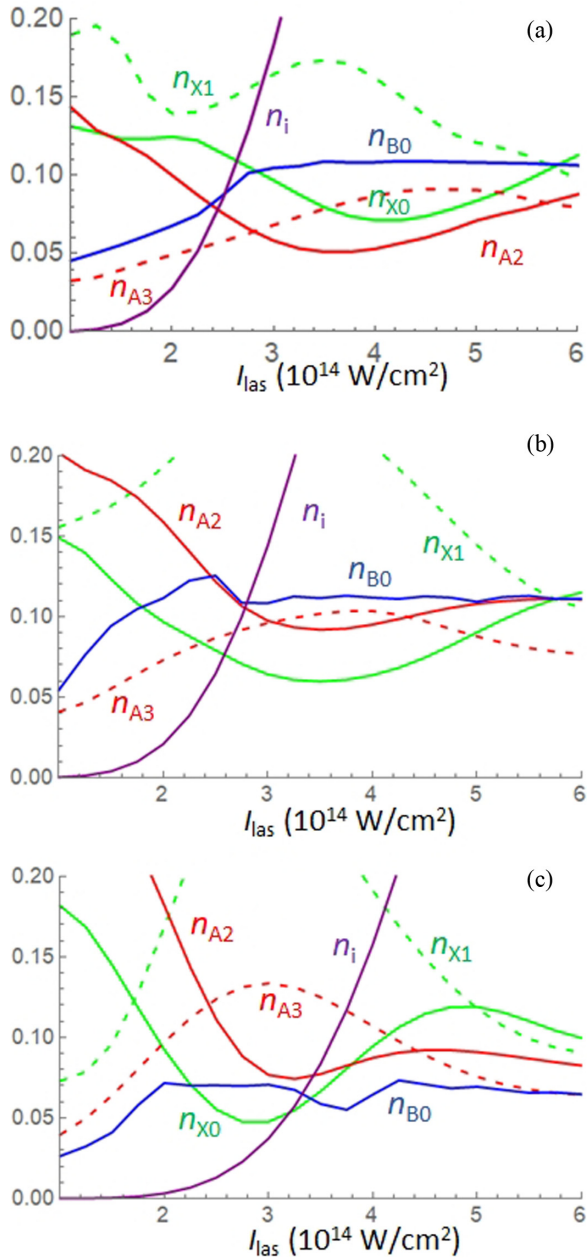


FIG. 9. Dependence of the populations in levels X0 (green solid line), X1 (green, dashed line), A2 (red solid line), A3 (red dashed line), and B0 (blue solid line) on laser intensity for a wavelength of 800 nm and a pulse duration of 30 fs. (a) Linear polarization, (b) $\epsilon = 0.4$, and (c) circular polarization. Curves A2 and A3 report cumulative populations in the right- and left-handed states.

levels. Positive ellipticity $\epsilon = 1$ favors a transition to states with $m = -1$. A significant level of excitation is achieved already at the laser-pulse maximum and evolves further in the second half of the pulse.

The efficiency of the ion transition to excited states depends on polarization. As ellipticity increases, the rate of transitions to the A states increases, while the populations in the B states decrease. Figure 9 shows the intensity dependence of populations in excited states for linear, elliptical ($\epsilon = 0.4$),

and circular polarizations. The case of linear polarization is the same as in Fig. 3(a), but only five levels are shown here.

Thus, our analysis shows that circular laser polarization is less suitable for excitation of the B states. It is more efficient at coupling X and A states that correspond to magnetic quantum numbers $m = \pm 1$. This conclusion is supported by studies of the dependence of populations in excited states on laser-pulse duration (in the range of 10–50 fs) and wavelength (in the range of 750–850 nm) for circular polarization. The populations in the B levels are limited to 5%–7%, while the populations in the X and A states vary in the range of 5%–20%. In some cases an inversion between A and B states is observed.

IV. CONCLUSIONS

We conducted an extensive analysis of ionization and excitation of nitrogen molecules with a high-amplitude, short laser pulse at a wavelength around 800 nm. The values of populations depend strongly on laser parameters and also on the number of considered excited levels. A sufficiently complete description was achieved by considering 11–13 levels covering a range of wavelengths from 300 to 1200 nm. This includes 2–3 vibrational levels in the ground state, 4–5 levels in the A state, and 4–5 levels in the B state.

A theoretical approach based on the density-matrix formalism has an advantage compared to the equations for the probability amplitudes by accounting, at the same time, for the ionization and excitation processes. It is therefore quantitatively more accurate for and capable of predicting population dependence on laser intensity, wavelength, and pulse duration.

The ionization model proposed by Tong *et al.* [35] agrees well with the experimental data. The ionization probability is reduced by a constant factor of 10 due to averaging over the radial intensity profile of the laser pulse. Ionization to the ground level X0 dominates. Excitation to higher electronic and vibrational levels is due to a dipole coupling of excited levels to the ground state in a strong laser electric field. For a linearly polarized laser pulse, transitions to the B state dominate. This is explained by the preference for transitions with the same magnetic quantum number, $m = 0$. By contrast, a circularly polarized laser pulse favors transitions with $\Delta m = \pm 1$, which leads to an increase of populations in the A states and decrease in the B states.

We found, however, a significant quantitative difference in the populations presented in Ref. [26], where the authors used a very similar approach, except for the angle averaging. The origins of this difference need further investigation. Averaging the results over molecule orientation with respect to the laser field orientation is an important part of the model. By choosing the appropriate orientation one may enable or disable B-X and A-X transitions and therefore incorrectly evaluate the population partition. We performed averaging by assuming an isotropic molecule distribution. It would be interesting to control the populations by using an aligned nitrogen gas in experiments.

The ionization-excitation model predicts a robust inversion between B and A states in the broad range of laser intensities and pulse durations considered. By contrast, population

inversion between $B0$ and $X0$ and X levels with vibrational numbers $v \geq 1$ was found to exist in only a very limited range of parameters. This fact indicates that amplification without inversion in the V scheme is the most plausible explanation of the observed $B0$ - $X0$ and $B0$ - $X1$ emissions at 391 and 428 nm [13].

ACKNOWLEDGMENTS

This work is supported in part by the National Natural Science Foundation of China (Grant No. 12034013) and the Innovation Program of the Shanghai Municipal Education Commission (Grant No. 2017-01-07-00-07-E00007).

APPENDIX: PARAMETERS OF THE NITROGEN MOLECULAR ION

Dipole moments are expressed in atomic units ea_B . According to Eq. (12), expressions for the dipole moment through the Einstein coefficient read

$$\mu_{ab} = 0.99 \times 10^{-3} (A_{ab} \lambda_{ab}^3)^{1/2}, \quad (\text{A1})$$

where A_{ab} is in s^{-1} and the wavelength λ_{ab} is in microns. Table I gives the wavelengths of the considered transitions along with the corresponding Einstein coefficients. Table II gives coefficients for N_2 molecule ionization.

-
- [1] J. Yao, G. Li, C. Jing, B. Zeng, W. Chu, J. Ni, H. Zhang, H. Xie, C. Zhang, H. Li, H. Xu, S. L. Chin, Y. Cheng, and Z. Xu, Remote creation of coherent emissions in air with two-color ultrafast laser pulses, *New J. Phys.* **15**, 023046 (2013).
- [2] Y. Liu, Y. Brelet, G. Point, A. Houard, and A. Mysyrowicz, Self-seeded lasing action of air pumped by 800 nm femtosecond laser pulses, *Opt. Express* **21**, 22791 (2013).
- [3] G. Li, C. Jing, B. Zeng, H. Xie, J. Yao, W. Chu, J. Ni, H. Zhang, H. Xu, Y. Cheng, and Z. Xu, Signature of superradiance from a nitrogen-gas plasma channel produced by strong-field ionization, *Phys. Rev. A* **89**, 033833 (2014).
- [4] G. Point, Y. Liu, Y. Brelet, S. Mitryukovskiy, P. J. Ding, A. Houard, and A. Mysyrowicz, Lasing of ambient air with microjoule pulse energy pumped by a multi-terawatt femtosecond laser, *Opt. Lett.* **39**, 1725 (2014).
- [5] H. Xu, E. Lötstedt, A. Iwasaki, and K. Yamanouchi, Sub-10-fs Population Inversion in N_2^+ in Air Lasing through Multiple State Coupling, *Phys. Rev. Lett.* **125**, 053201 (2020).
- [6] J. Yao, S. Jiang, W. Chu, B. Zeng, C. Wu, R. Lu, Z. Li, H. Xie, G. Li, C. Yu, Z. Wang, H. Jiang, Q. Gong, and Y. Cheng, Population Redistribution among Multiple Electronic States of Molecular Nitrogen Ions in Strong Laser Fields, *Phys. Rev. Lett.* **116**, 143007 (2016).
- [7] Y. Zhang, E. Lötstedt, and K. Yamanouchi, Population inversion in a strongly driven two-level system far-off resonance, *J. Phys. B* **50**, 185603 (2017).
- [8] M. Britton, P. Laferrière, D. H. Ko, Z. Li, F. Kong, G. Brown, A. Naumov, C. Zhang, L. Arissian, and P. B. Corkum, Testing the Role of Recollision in N_2^+ Air Lasing, *Phys. Rev. Lett.* **120**, 133208 (2018).
- [9] M. Britton, M. Lytova, P. Laferrière, P. Peng, F. Morales, D. H. Ko, M. Richter, P. Polynkin, D. M. Villeneuve, C. Zhang, M. Ivanov, M. Spanner, L. Arissian, and P. B. Corkum, Short- and long-term gain dynamics in N_2^+ air lasing, *Phys. Rev. A* **100**, 013406 (2019).
- [10] Y. Liu, P. Ding, G. Lambert, A. Houard, V. T. Tikhonchuk, and A. Mysyrowicz, Recollision-Induced Superradiance of Ionized Nitrogen Molecules, *Phys. Rev. Lett.* **115**, 133203 (2015).
- [11] V. T. Tikhonchuk, J.-F. Tremblay-Bugeaud, Y. Liu, A. Houard, and A. Mysyrowicz, Excitation of nitrogen molecular ions in a strong laser field by electron recollisions, *Europ. J. Phys. D* **71**, 292 (2017).
- [12] V. T. Tikhonchuk, Y. Liu, R. Danylo, A. Houard, and A. Mysyrowicz, Theory of femtosecond strong field ion excitation and subsequent lasing in N_2^+ , *New J. Phys.* **23**, 023035 (2021).
- [13] A. Mysyrowicz, R. Danylo, A. Houard, V. Tikhonchuk, X. Zhang, Z. Fan, Q. Liang, S. Zhuang, L. Yuan, and Y. Liu, Lasing without population inversion in N_2^+ , *APL Photonics* **4**, 110807 (2019).
- [14] O. A. Kocharovskaya and Ya. I. Khanin, Coherent amplification of an ultrashort pulse in a three-level medium without a population inversion, *JETP Lett.* **48**, 630 (1988).
- [15] S. E. Harris, Lasers without Inversion: Interference of Lifetime-Broadened Resonances, *Phys. Rev. Lett.* **62**, 1033 (1989).
- [16] M. O. Scully, S.-Y. Zhu, and A. Gavrielides, Degenerate Quantum-Beat Laser: Lasing without Inversion and Inversion without Lasing, *Phys. Rev. Lett.* **62**, 2813 (1989).
- [17] A. A. Svidzinsky, L. Yuan, and M. O. Scully, Transient lasing without inversion, *New J. Phys.* **15**, 053044 (2013).
- [18] J. Mompert, C. Peters, and R. Corbalan, Interpretation of transient V scheme amplification without inversion, *Quantum Semiclass. Opt.* **10**, 355 (1998).
- [19] V. A. Malyshev, I. V. Ryzhov, E. D. Trifonov, and A. I. Zaitsev, Superradiance without inversion, *Laser Phys.* **8**, 494 (1998).
- [20] V. V. Kozlov, P. G. Polynkin, and M. O. Scully, Resonant raman amplification of ultrashort pulses in a V -type medium, *Phys. Rev. A* **59**, 3060 (1999).
- [21] H. Zhang, C. Jing, J. Yao, G. Li, B. Zeng, W. Chu, J. Ni, H. Xie, H. Xu, S. L. Chin, K. Yamanouchi, Y. Cheng, and Z. Xu, Rotational Coherence Encoded in an “Air-Laser” Spectrum of Nitrogen Molecular Ions in an Intense Laser Field, *Phys. Rev. X* **3**, 041009 (2013).
- [22] M. Richter, M. Lytova, F. Morales, S. Haessler, O. Smirnova, M. Spanner, and M. Ivanov, Rotational quantum beat lasing without inversion, *Optica* **7**, 586 (2020).
- [23] M. Lytova, M. Richter, F. Morales, O. Smirnova, M. Ivanov, and M. Spanner, N_2^+ lasing: Gain and absorption in the presence of rotational coherence, *Phys. Rev. A* **102**, 013111 (2020).
- [24] S. R. Langhoff, Jr., C. W. Bauschlicher, and H. Partridge, Theoretical study of the N_2^+ Meinel system, *J. Chem. Phys.* **87**, 4716 (1987).
- [25] S. R. Langhoff and C. W. Bauschlicher, Jr., Theoretical study of the first and second negative systems of N_2^+ , *J. Chem. Phys.* **88**, 329 (1988).

- [26] Q. Zhang, H. Xie, G. Li, X. Wang, H. Lei, J. Zhao, Z. Chen, J. Yao, Y. Cheng, and Z. Zhao, Sub-cycle coherent control of ionic dynamics via transient ionization injection, *Commun. Phys.* **3**, 50 (2020).
- [27] D. C. Jain and R. C. Sahni, Einstein coefficients, cross sections, f values, dipole moments, and all that, *Int. J. Quantum Chem.* **1**, 721 (1967).
- [28] A. Lofthus and P. H. Krupenie, The spectrum of molecular nitrogen, *J. Phys. Chem. Ref. Data* **6**, 113 (1977).
- [29] Y. Fu, E. Lötstedt, H. Li, S. Wang, D. Yao, T. Ando, A. Iwasaki, F. H. M. Faisal, K. Yamanouchi, and H. Xu, Optimization of N_2^+ lasing through population depletion in the $X_2\sigma_g^+$ state using elliptically modulated ultrashort intense laser fields, *Phys. Rev. Research* **2**, 012007(R) (2020).
- [30] J. Chen, J. Yao, H. Zhang, Z. Liu, B. Xu, W. Chu, L. Qiao, Z. Wang, J. Fatome, O. Faucher, C. Wu, and Y. Cheng, Electronic-coherence-mediated molecular nitrogen-ion lasing in a strong laser field, *Phys. Rev. A* **100**, 031402(R) (2019).
- [31] R. C. Hilborn, Einstein coefficients, cross sections, f values, dipole moments, and all that, *Am. J. Phys.* **50**, 982 (1982).
- [32] A. M. Perelomov, V. S. Popov, and M. V. Terent'ev, Ionization of atoms in an alternating electric field, *Sov. Phys. JETP* **23**, 924 (1966).
- [33] M. V. Ammosov, N. B. Delone, and V. P. Krainov, Tunnel ionization of complex atoms and atomic ions in electromagnetic field, *Sov. Phys. JETP* **64**, 1191 (1986).
- [34] V. S. Popov, Tunnel and multiphoton ionization of atoms and ions in a strong laser field (Keldysh theory), *Phys. Usp.* **47**, 855 (2004).
- [35] X. M. Tong, Z. X. Zhao, and C. D. Lin, Theory of molecular tunneling ionization, *Phys. Rev. A* **66**, 033402 (2002).
- [36] L. D. Landau and E. M. Lifshitz, *Quantum Mechanics: Non-relativistic Theory*, Course of Theoretical Physics Vol. 3, (Butterworth-Heinemann, Oxford, 1977).
- [37] S. Petretti, Y. V. Vanne, A. Saenz, A. Castro, and P. Decleva, Alignment-Dependent Ionization of N_2 , O_2 , and CO_2 in Intense Laser Fields, *Phys. Rev. Lett.* **104**, 223001 (2010).
- [38] C. Guo, M. Li, J. P. Nibarger, and G. N. Gibson, Single and double ionization of diatomic molecules in strong laser fields, *Phys. Rev. A* **58**, R4271 (1998).